Ethylene Complexes of the Early Transition Metals: Crystal Structures of $[HfEt_4(C_2H_4)^{2-}]$ and the Negative-Oxidation-State Species $[TaHEt(C_2H_4)_3^{3-}]$ and $[WH(C_2H_4)_4^{3-}]$

Paige M. Morse, Quinetta D. Shelby, Do Young Kim, and Gregory S. Girolami*

School of Chemical Sciences, University of Illinois at Urbana−Champaign, 600 South Mathews Avenue, Urbana, Illinois 61801

Received November 27, 2007

Alkylation of $HfCl_4$ with 6 equiv of ethyllithium followed by the addition of *N*,*N*,*N*′,*N*′-tetramethylethylenediamine gives the d^2 hafnium(II) alkyl/alkene complex $[Li(tmed)]_2[HfEt_4(C_2H_4)]$. The X-ray crystal structure of this complex shows that the ethylene ligand has considerable metallacyclopropane character. The C−C distance of 1.49(6) Å and the $^1J_{CH}$ coupling constant of 119 Hz both support this formulation. A labeling study showed that the ethylene ligand is formed by means of a β-hydrogen abstraction process. Similar treatment of $TaCl_2(OMe)_3$ and $WCl_3(OMe)_3$ with ethyllithium affords the d^6 tantalum(−I) and d^8 tungsten(−II) complexes $[Li(tmed)]_3[TaHEt(C_2H_4)_3]\cdot{}^1/_2$tmed and $[Li(tmed)]_3[WH(C_2H_4)_4]$. Both trianionic complexes, in which the metal centers have negative oxidation states, adopt distorted-square-pyramidal geometries with the hydride group in the axial position. The C−C bond lengths of 1.484(8), 1.502(8), and 1.515(8) Å for the ethylene groups in the tantalum complex are somewhat longer than those of 1.357(11)–1.466(10) Å in the tungsten complex. In both complexes, the Ta−H and W−H bonds are relatively long at 2.07(9) and 2.04(5) Å, due to the presence of close contacts with two lithium cations. In both the tantalum and tungsten complexes, two of the ethylene ligand(s) are involved in interactions with the lithium cations; these ethylene ligands rotate slowly about their metal–ligand axes on the NMR time scale at −80 °C, whereas at this temperature the remaining ethylene ligands are rotating rapidly. At higher temperatures, the inequivalence of the ethylene environments is maintained in the tantalum complex, but they exchange in the tungsten compound. The activation parameters for the latter process are $\Delta H^{\ddagger} = 9.5(10)$ kcal mol^{-1} and $\Delta S^{\ddagger} = -5(4)$ cal mol^{-1} K^{-1}. Spin saturation transfer experiments show that there is no exchange of the W−H and W−C_2H_4 environments on the NMR time scale. Qualitative molecular orbital descriptions of the bonding in all three compounds are presented.

Introduction

Complexes of transition metals in negative oxidation states have exerted a fascination since Blanchard first proposed the concept in reference to the binary metal–carbonyl anions $[Fe(CO)_4^{2-}]$ and $[Co(CO)_4^{-}]$.[1] Since that time, the majority of transition-metal complexes in negative oxidation states have been metal carbonyls, a topic that has been explored in great detail by Ellis.[2–5] Today, such compounds are known for almost every metal in the d block between group 4 and group 10. The lowest known oxidation state for any transition metal is −4, which is found in the group 6 tetracarbonylmetalate complexes $[M(CO)_4^{4-}]$, where M is Cr, Mo, or W.[6] Another particularly notable accomplishment in this area was the extension of the d^6 metal hexacarbonyl series to the group 4 anions $[M(CO)_6^{2-}]$, where M is Ti, Zr, or Hf.[7]

Besides carbon monoxide, relatively few two-electron donors are capable of forming binary complexes of transition metals in negative oxidation states. Cooper was the first to show that organic isonitriles, which are close analogues of carbon monoxide except they are more strongly donating, can form such complexes. The first examples were $[Co(CNXyl)_4^{-}]$,[8] $[Ru(CN\text{-}t\text{-}Bu)_4^{2-}]$,[9] and $[Mn(CNXyl)_5^{-}]$,[10] and more recently this class was augmented by the isolation of $[Fe(CNXyl)_4^{2-}]$,[11] $[V(CNXyl)_6^{-}]$,[12] $[Nb(CNXyl)_6^{-}]$,[13] and $[Ta(CNXyl)_6^{-}]$.[13] Largely through the work of Kruck, several trifluorophosphine complexes of metals in negative oxidation states are known: the group 9 complexes $[M(PF_3)_4^{-}]$, where M is Co, Rh, or Ir,[14] the group 8 complexes $[M(PF_3)_4^{2-}]$, where M is Fe, Ru, or Os,[15,16] the group 7 complexes $[M(PF_3)_5^{-}]$, where M is Mn or Re,[17] and the group 5 complex $[M(PF_3)_6^{-}]$, where M is V, Nb, or

(1) Blanchard, A. A. *Chem. Rev.* **1940**, *26*, 409–422.
(2) Beck, W. *Angew. Chem., Int. Ed. Engl.* **1991**, *30*, 168–169.
(3) Ellis, J. E. *Adv. Organomet. Chem.* **1990**, *31*, 1–51.
(4) Ellis, J. E. *Organometallics* **2003**, *22*, 3322–3338.
(5) Ellis, J. E. *Inorg. Chem.* **2006**, *45*, 3167–3186.
(6) Lin, J. T.; Hagen, G. P.; Ellis, J. E. *J. Am. Chem. Soc.* **1983**, *105*, 2296–2303.
(7) Ellis, J. E.; Chi, K.-M. *J. Am. Chem. Soc.* **1990**, *112*, 6022–6025.
(8) Leach, P. A.; Geib, S. J.; Corella, J. A., II; Warnock, G. F.; Cooper, N. J *J. Am. Chem. Soc.* **1994**, *116*, 8566–8574.
(9) Corella, J. A., II; Thompson, R. L.; Cooper, N. J *Angew. Chem., Int. Ed. Engl.* **1992**, *31*, 83–84.
(10) Utz, T. L.; Leach, P. A.; Geib, S. J.; Cooper, N. J. *Chem. Commun.* **1997**, *847*, 848.
(11) Brennessel, W. W.; Ellis, J. E. *Angew. Chem., Int. Ed.* **2007**, *46*, 598–600.
(12) Barybin, M. V.; Young, V. G., Jr.; Ellis, J. E. *J. Am. Chem. Soc.* **2000**, *122*, 4678–4691.
(13) Barybin, M. V.; Brennessel, W. W.; Kucera, B. E.; Minyaev, M. E.; Sussman, V. J.; Young, V. G.; Ellis, J. E *J. Am. Chem. Soc.* **2007**, *129*, 1141–1150.
(14) Kruck, T.; Lang, W.; Derner, N.; Stadler, M. *Chem. Ber.* **1968**, *101*, 3816–3826.
(15) Kruck, T.; Engelmann, A. *Angew. Chem., Int. Ed. Engl.* **1966**, *5*, 836.
(16) Kruck, T.; Prasch, A. *Z. Anorg. Allg. Chem.* **1969**, *371*, 1–22.
(17) Kruck, T.; Kobelt, R. *Chem. Ber.* **1972**, *105*, 3772–2782.

10.1021/om701189e CCC: $40.75
Publication on Web 02/15/2008

Ta.[18–21]Triorganophosphines and triorgano phosphites are also capable of stabilizing metals in negative oxidation states, but here the scope is rather limited, the only known examples being the cobalt(−I) complexes $[Co(PMe_3)_4^-]$[22] and $[Co\{P(OMe)_3\}_4^-]$.[23]

The ability of a two electron donor to stabilize transition metals in negative oxidation states is closely related to its π-accepting ability. The importance of π-back-bonding in metal–ligand interactions was, of course, first articulated by Dewar and by Chatt and Duncanson in reference to metal−alkene complexes.[24,25] Interestingly, however, and ironically, despite the fact that ethylene is a reasonably strong π-acceptor, only three examples of binary ethylene complexes in negative oxidation states are known: $[Ni(C_2H_4)_3^{2-}]$, $[Co(C_2H_4)_4^-]$, and $[Fe(C_2H_4)_4^{2-}]$. Only the last compound has been crystallographically characterized.[26]

We wondered whether binary ethylene complexes of early transition metals could be obtained by addition of ethyllithium to early-transition-metal halides, taking advantage of β-hydrogen elimination both to generate the ethylene ligands and to reduce the metal to lower oxidation states by means of reductive elimination steps. Such an approach would be an extension of the synthesis of "permethyl" complexes by addition of methyllithium to early-transition-metal halides. We previously reported one of the most interesting examples of such permethyl complexes, the hexamethylzirconate dianion $[ZrMe_6^{2-}]$, which adopts a trigonal-prismatic geometry owing to a second order Jahn–Teller effect.[27] We now report the isolation of unusual ethylene complexes of d^2 hafnium(II), d^6 tantalum(−I), and d^8 tungsten(−II) by alkylations of the corresponding metal salts with ethyllithium. Portions of this work have been reported previously.[28,29]

Results and Discussion

Anionic Ethylene Complex of Hafnium. The alkylation of $HfCl_4$ with 6 equiv of ethyllithium followed by the addition of 2 equiv of *N*,*N*,*N*′,*N*′-tetramethylethylenediamine (tmed) yields the unique hafnium ethyl/ethylene complex $[Li(tmed)]_2[Hf(C_2H_4)Et_4]$.

$$HfCl_4 + 6LiEt + 2tmed \rightarrow \underset{\mathbf{1}}{[Li(tmed)]_2[Hf(C_2H_4)Et_4]} + 4LiCl + C_2H_6$$

Attempts to make the analogous zirconium complex led to red-orange solutions that did not yield a pure product. The off-white, pyrophoric complex $[Li(tmed)]_2[Hf(C_2H_4)Et_4]$ decomposes at ca. 100 °C under an inert atmosphere.

Table 1. Crystal Data for $[Li(tmed)]_2[HfEt_4(C_2H_4)]$ (1), $[Li(tmed)]_3[TaHEt(C_2H_4)_4]\cdot{}^1/_2$tmed (2), and $[Li(tmed)]_3[WH(C_2H_4)_4]$ (3)

	1	2	3
formula	$HfC_{22}H_{56}Li_2N_4$	$TaC_{29}H_{74}Li_3N_7$	$WC_{26}H_{65}Li_3N_6$
formula wt	569.08	717.68	666.51
T, °C	−80	−80	−75
space group	*Pbca*	$P2_1/c$	*Pbca*
a, Å	21.610(3)	18.318(10)	15.3935(4)
b, Å	17.342(2)	13.333(7)	13.3225
c, Å	32.154(4)	16.650(9)	34.6471(6)
α, deg	90	90	90
β, deg	90	102.542(9)	90
γ, deg	90	90	90
V, Å^3	12051(3)	3970(4)	7105.4(3)
Z	16	4	8
ρ_{calcd}, g cm^{-3}	1.255	1.201	1.246
λ, Å	0.71073	0.71073	0.71073
μ_{calcd}, cm^{-1}	34.75	27.93	32.72
transmission coeff	0.614–0.675	0.266–0.545	0.510–0.801
$R(F)^a$	0.0242	0.0404	0.0531
$R_w(F^2)^b$	0.0683	0.0899	0.1533

[a] $R(F) = \sum||F_o| - |F_c||/\sum|F_o|$ for reflections with $F_o^2 > 2\sigma(F_o^2)$. [b] $R_w(F^2) = [\sum w(F_o^2 - F_c^2)^2/\sum w(F_o^2)^2]^{1/2}$ for all reflections.

The ethylene ligand in **1** must be generated by loss of a hydrogen atom from a Hf−ethyl group. This conversion could occur in two different ways: by β-elimination or by α-elimination followed by rearrangement of the resulting ethylidene ligand to an ethylene group. Because early-transition-metal alkyls that are not β-stabilized sometimes undergo α-elimination and β-elimination with comparable rates,[30–34] the two possibilities were tested by treating $HfCl_4$ with $LiCH_2CD_3$. The evolved gases were analyzed by GC/MS and were found to consist predominantly of d_4-ethane. This result clearly shows that β-elimination is the principal reaction pathway by which **1** is formed.

Crystal data for **1** are presented in Table 1, Table 2, and selected bond distance and angles are collected in Table 3. The unit cell contains two crystallographically independent molecules, and the overall geometries of the two independent molecules are very similar. The molecular structure of **1** most closely resembles that of a square pyramid with the CH_2CH_2 ligand at the apex and the four ethyl groups at the basal sites (Figure 2). The ethylene ligand and two of the Hf−Et bonds are coplanar, and these two Et groups are displaced significantly out of the idealized square plane toward the unoccupied site of the square pyramid. The C−Hf−C angle between these two ethyl groups is 131.4(1)° vs 150.0(1)° for the other two ethyl groups.

The hafnium−carbon distances to the ethyl groups are 2.38–2.45 Å, whereas the Hf−C distances to the ethylene carbon atoms of 2.26–2.33 Å are significantly shorter. The carbon−carbon distances within the ethyl groups are about the same length (1.50–1.56 Å) as the carbon−carbon distance in the ethylene ligand (1.52(8) and 1.49(6) Å), which suggests that the ethylene

(18) Collong, W.; Kruck, T. *Chem. Ber.* **1990**, *123*, 1655–1656.
(19) Barybin, M. V.; Pomije, M. K.; Ellis, J. E. *Inorg. Chim. Acta* **1998**, *269*, 58–62.
(20) Barybin, M. V.; Ellis, J. E.; Pomije, M. K.; Tinkham, M. L.; Warnock, G. F. *Inorg. Chem.* **1998**, *37*, 6518–6527.
(21) Ellis, J. E.; Warnock, G. F.; Barybin, M. V.; Pomije, M. K *Chem. Eur. J.* **1995**, *1*, 521–527.
(22) Hammer, R.; Klein, H. F. *Z. Naturforsch., B* **1977**, *32B*, 138–143.
(23) Muetterties, E. L.; Hirsekorn, F. J. *J. Am. Chem. Soc.* **1974**, *96*, 7920–7926.
(24) Dewar, M. J. S. *Bull. Soc. Chim. Fr.* **1951**, *18*, C71–C79.
(25) Chatt, J.; Duncanson, L. A. *J. Chem. Soc.* **1953**, *2939*, 2947.
(26) Jonas, K.; Schieferstein, L.; Krüger, C.; Tsay, Y-H. *Angew. Chem., Int. Ed. Engl.* **1979**, *18*, 550–551.
(27) Morse, P. M.; Girolami, G. S. *J. Am. Chem. Soc.* **1989**, *111*, 4114–4116.
(28) Spencer, M. D.; Morse, P. M.; Wilson, S. R.; Girolami, G. S. *J. Am. Chem. Soc.* **1993**, *115*, 2057–2059.
(29) Shelby, Q. D.; Girolami, G. S. *Organometallics* **1999**, *18*, 2297–2299.
(30) Fellmann, J. D.; Schrock, R. R.; Traficante, D. D. *Organometallics* **1982**, *1*, 481–484.
(31) Parkin, G.; Bunel, E.; Burger, B. J.; Trimmer, M. S.; Van Asselt, A.; Bercaw, J. E. *J. Mol. Catal.* **1987**, *41*, 21–39.
(32) Carmona, E.; Paneque, M.; Poveda, M. L. *Dalton Trans.* **2003**, 4022–4029.
(33) Paneque, M.; Poveda, M. L.; Santos, L. L.; Carmona, E.; Lledos, A.; Ujaque, G.; Mereiter, K. *Angew. Chem., Int. Ed.* **2004**, *43*, 3708–3711.
(34) Kuznetsov, V. F.; Abdur-Rashid, K.; Lough, A. J.; Gusev, D. G. *J. Am. Chem. Soc.* **2006**, *128*, 14388–14396.

Table 2. Selected Bond Distances and Angles for [Li(tmed)]$_2$[HfEt$_4$(C$_2$H$_4$)] (1)

Bond Lengths (Å)			
Hf(1)−C(11)	2.318(4)	C(17)−H(17A)	0.980(10)
Hf(1)−C(13)	2.372(3)	C(17)−H(17B)	0.970(10)
Hf(1)−C(15)	2.380(4)	C(19)−H(19A)	0.862(11)
Hf(1)−C(17)	2.288(4)	C(19)−H(19B)	0.855(11)
Hf(1)−C(19)	2.264(4)	C(20)−H(20A)	0.864(11)
Hf(1)−C(20)	2.271(3)	C(20)−H(20B)	0.867(11)
Hf(1)−Li(1)	2.938(5)	Li(1)−C(15)	2.221(6)
Hf(1)−Li(2)	2.931(5)	Li(1)−C(19)	2.172(6)
C(11)−C(12)	1.509(5)	Li(2)−C(13)	2.224(6)
C(13)−C(14)	1.532(4)	Li(2)−C(20)	2.184(6)
C(15)−C(16)	1.521(4)	Li(1)−H(15A)	1.94(3)
C(17)−C(18)	1.511(6)	Li(1)−H(15B)	2.17(3)
C(19)−C(20)	1.509(5)	Li(1)−H(19A)	2.23(3)
C(11)−H(11A)	0.962(9)	Li(1)−H(19B)	2.15(3)
C(11)−H(11B)	0.974(9)	Li(2)−H(13A)	2.18(2)
C(13)−H(13A)	0.968(9)	Li(2)−H(13B)	1.97(3)
C(13)−H(13B)	0.965(9)	Li(2)−H(20A)	2.18(3)
C(15)−H(15A)	0.969(9)	Li(2)−H(20B)	2.33(3)
C(15)−H(15B)	0.964(10)		
Bond Angles (deg)			
C(19)−Hf(1)−C(20)	38.87(12)	C(19)−Hf(1)−C(17)	102.67(18)
C(11)−Hf(1)−C(13)	83.00(15)	C(20)−Hf(1)−C(11)	100.44(15)
C(11)−Hf(1)−C(15)	83.26(15)	C(20)−Hf(1)−C(13)	95.55(12)
C(13)−Hf(1)−C(15)	131.43(12)	C(20)−Hf(1)−C(15)	132.75(12)
C(17)−Hf(1)−C(11)	150.03(16)	C(20)−Hf(1)−C(17)	107.74(17)
C(17)−Hf(1)−C(13)	84.31(16)	C(12)−C(11)−Hf(1)	113.8(3)
C(17)−Hf(1)−C(15)	85.02(17)	C(14)−C(13)−Hf(1)	102.7(2)
C(19)−Hf(1)−C(11)	105.66(17)	C(18)−C(17)−Hf(1)	112.5(3)
C(19)−Hf(1)−C(13)	134.15(13)	C(19)−C(20)−Hf(1)	70.33(19)
C(19)−Hf(1)−C(15)	94.43(12)	C(20)−C(19)−Hf(1)	70.81(19)

Table 3. Selected Bond Distances and Angles for [Li(tmed)]$_3$[TaHEt(C$_2$H$_4$)$_4$]·$^1/_2$tmed (2)

Bond Lengths (Å)			
Ta−H	2.07(6)	C(3)−C(4)	1.484(9)
Ta−C(1A)	2.319(15)	C(5)−C(6)	1.515(8)
Ta−C(3)	2.249(7)	C(7)−C(8)	1.502(8)
Ta−C(4)	2.270(7)	Li(2)−H	1.99(7)
Ta−C(5)	2.251(7)	Li(3)−H	1.92(6)
Ta−C(6)	2.286(7)	Li(1)−C(3)	2.502(15)
Ta−C(7)	2.256(6)	Li(1)−C(5)	2.331(15)
Ta−C(8)	2.290(6)	Li(1)−C(7)	2.229(15)
Ta−Li(1)	2.699(12)	Li(2)−C(4)	2.608(13)
Ta−Li(2)	2.772(11)	Li(2)−C(6)	2.316(15)
Ta−Li(3)	2.823(11)	Li(3)−C(4)	3.17
C(1A)−C(2A)	1.510(13)	Li(3)−C(8)	2.232(15)
Bond Angles (deg)			
C(3)−Ta−C(1A)	171.1(4)	C(6)−Ta−C(8)	178.5(3)
C(3)−Ta−C(4)	38.3(2)	C(7)−Ta−C(1A)	87.5(4)
C(3)−Ta−C(5)	87.0(3)	C(7)−Ta−C(4)	109.0(3)
C(3)−Ta−C(6)	88.9(3)	C(7)−Ta−C(6)	140.8(2)
C(3)−Ta−C(7)	85.4(3)	C(7)−Ta−C(8)	38.6(2)
C(3)−Ta−C(8)	89.6(3)	C(8)−Ta−C(1A)	88.2(5)
C(4)−Ta−C(1A)	150.2(4)	C(1A)−Ta−H	65.5(18)
C(4)−Ta−C(6)	89.1(3)	C(3)−Ta−H	123.2(18)
C(4)−Ta−C(8)	90.0(3)	C(4)−Ta−H	84.8(18)
C(5)−Ta−C(1A)	89.3(4)	C(5)−Ta−H	122.7(17)
C(5)−Ta−C(4)	110.3(3)	C(6)−Ta−H	89.5(18)
C(5)−Ta−C(6)	39.0(2)	C(7)−Ta−H	125.6(18)
C(5)−Ta−C(7)	101.9(2)	C(8)−Ta−H	91.7(18)
C(5)−Ta−C(8)	140.5(2)	Ta−C(1A)−C(2A)	121.2(9)
C(6)−Ta−C(1A)	93.2(5)		

ligand is best viewed as a metallacyclopropane rather than a π-bound ethylene complex.

There are a reasonable number of hafnium ethyl complexes of the type $(C_5R_5)_2HfEt(L)$, where L is a variety of anionic and neutral donor ligands, four of which have been crystallographically characterized: $Cp_2HfEt(CH{=}PPh_3)$,[35] $Cp_2HfEt(OOCMe_3)$,[36] $Cp_2HfEt(OCCHPPh_3)$,[37] and $Cp_2HfEt(PhCH_2N{=}CHCH_2PPh_3)$.[38] There are a small number of non-metallocene hafnium ethyl complexes, two of which have been structurally characterized: the amide $HfEt_2[O(CH_2CH_2NC_6H_3\text{-}2,6\text{-}(i\text{-}Pr)_2)_2]$,[39] and the amidinate $HfEt_2[PhC(NSiMe_3)_2]$.[40] The hafnium−carbon distances to the ethyl groups of these compounds are slightly shorter, at 2.285(8) and 2.280(13) Å, respectively, than those in $[Li(tmed)]_2[Hf(C_2H_4)Et_4]$.

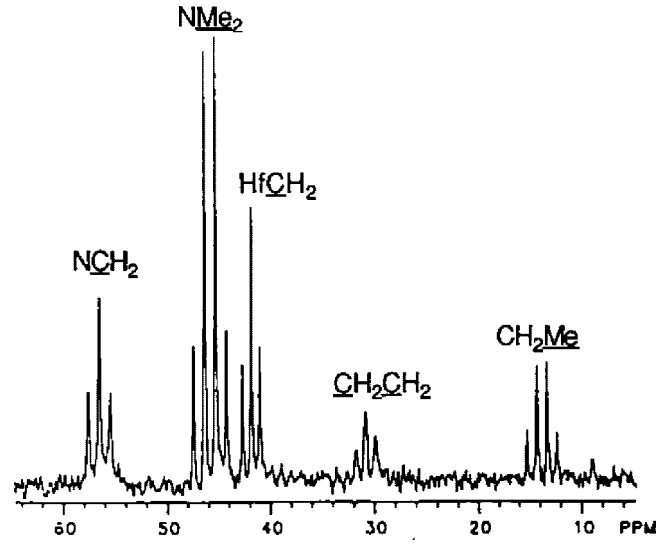

Figure 1. 300 MHz ^{13}C NMR spectrum of $[Li(tmed)]_2[Hf(C_2H_4)Et_4]$ (**1**) in C_6D_6 at 20 °C.

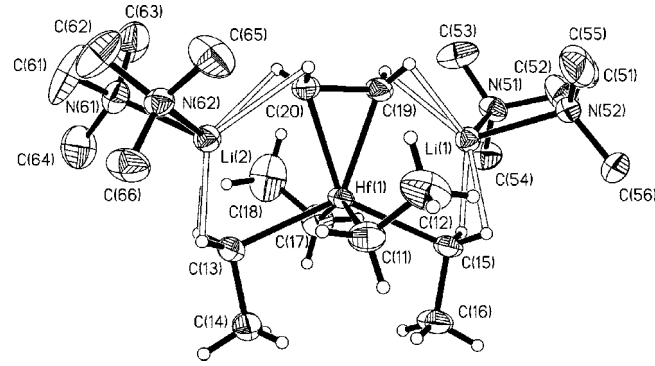

Figure 2. Molecular structure of $[Li(tmed)]_2[Hf(C_2H_4)Et_4]$ (**1**). The ellipsoids represent the 30% probability density surfaces, except for hydrogen atoms, which are represented by arbitrarily sized spheres.

The lithium atoms bridge between the ethylene carbons and the α-carbons of the adjacent ethyl groups. The most pronounced difference between the two independent molecules in the unit cell is that in one molecule the lithium atoms are closer to the ethyl carbons (2.05(8) and 2.04(10) Å) than to the ethylene carbons (2.40(9) and 2.37(10) Å), whereas in the other molecule

(35) Erker, G.; Czisch, P.; Krüger, C.; Wallis, J. M. *Organometallics* **1985**, *4*, 2059–2060.
(36) Van Asselt, A.; Santarsiero, B. D.; Bercaw, J. E. *J. Am. Chem. Soc.* **1986**, *108*, 8291–8293.
(37) Erker, G.; Korek, U.; Schlund, R.; Krüger, C. *J. Organomet. Chem.* **1989**, *364*, 133–147.
(38) Erker, G.; Korek, U.; Petersen, J. L. *J. Organomet. Chem.* **1988**, *355*, 121–138.
(39) Aizenberg, M.; Turculet, L.; Davis, W. M.; Schattenmann, F.; Schrock, R. R. *Organometallics* **1998**, *17*, 4795–4812.
(40) Fischer, R.; Walter, D.; Imhof, W. *Acta Crystallogr., Sect. E* **2006**, *62*, m568–m570.

they are approximately equidistant from the ethyl carbons (2.20(8) and 2.24(8) Å) and the ethylene carbons (2.27(8) and 2.27(7) Å).

Only one other mononuclear hafnium ethylene complex, $Cp_2Hf(C_2H_4)(PMe_3)$, has been reported.[41] The chemical shifts of the ethylene ligand in this complex (^{1}H NMR, δ −0.06, 0.19; ^{13}C NMR, δ 10.5, 14.3) are similar to those of the analogous (and structurally characterized) zirconium complex $Cp_2Zr(C_2H_4)(PMe_3)$.[42] Like compound **1**, the carbon−carbon bond length of 1.486(8) Å in the latter molecule is rather long and suggests that the compound has considerable metallacycle character. Another zirconium alkene complex, $Cp_2Zr(PhCH{=}CHPh)(PMe_3)$, has a C−C distance of 1.38(2) Å that is characteristic of a π-bound alkene.[43] Butadiene complexes of zirconium and hafnium have also been reported,[44] and the C−C bond lengths of ca. 1.40 Å are more typical of C−C double bonds. Hafnium compounds are known in which ethylene bridges between two hafnium centers in an η^2,η^2 manner.[45]

The ^{1}H NMR spectrum of **1** in C_6D_6 shows a singlet at δ 0.31 for the ethylene protons and a quartet at δ 0.05 (J_{HH} = 7.5 Hz) for the α-protons and a triplet at δ 2.06 (J_{HH} = 7.5 Hz) for the β-protons of the ethyl substituents. The ^{13}C NMR resonance for the ethylene carbons (δ 31.0) shows a C−H coupling constant of 120 Hz (Figure 1); in contrast, ethylene ligands bound to later transition metals typically have C−H coupling constants of 145−160 Hz.[46] This difference suggests that the C−H bonds of the ethylene ligand in **1** are sp^3-like, which supports the conclusion from the crystallographic data that this ligand is best viewed as a metallacyclopropane rather than a π-bound ethylene. The oxidation state of hafnium may be better regarded as +4, rather than +2. Consistent with this view, the ^{1}H and ^{13}C NMR chemical shifts and coupling constants for the ethyl groups of $[Li(tmed)]_2[Hf(C_2H_4)Et_4]$ are similar to those seen in hafnium(IV) ethyl complexes.[35−38,47−54] The principal difference is that α-proton resonance of the ethyl groups in **1** is farther upfield than those of electrically neutral hafnium(IV) compounds. This difference may reflect the presence of contacts with the lithium cations (see below). The $^{13}C\{^1H\}$ CPMAS NMR spectrum of **1** at −50 °C contains three resonances for the β-carbons of the ethyl groups in a 1:2:1 ratio and probably a similar number of peaks for the α-carbons, although several of the latter are probably obscured by the peaks due to the tmed ligands. Interestingly, the chemical shifts of the α-carbons in the solid state range from δ 34 to 52, vs the shift of δ 41 observed in solution. This result suggests that the shifts are strongly affected by whether or not the carbon atoms are interacting with the lithium centers.

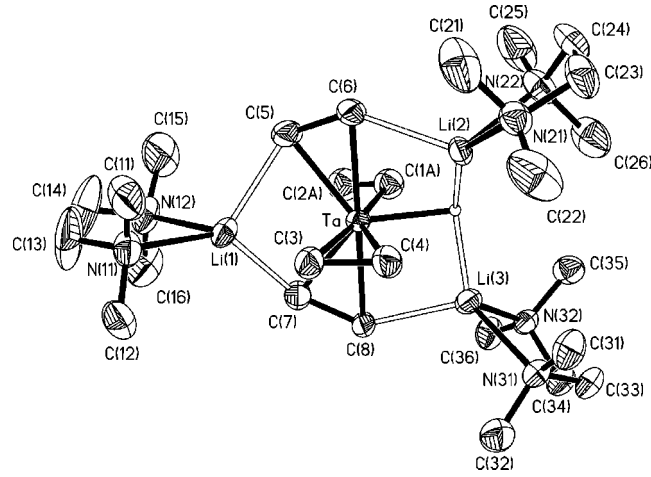

Figure 3. Molecular structure of $[Li(tmed)]_3[TaHEt(C_2H_4)_4]$ (**2**). The ellipsoids represent the 30% probability density surfaces, except for hydrogen atoms, which are represented by arbitrarily sized spheres. One position for the disordered ethyl group (C1A−C2A) is shown.

If the ethylene ligand in compound **1** is viewed as a metallacyclopropane, then the formal oxidation state of the Hf center is +4, and the diamagnetism of the complex is due to the d^0 electronic configuration. If instead the ethylene ligand is considered as a neutral group, then the formal oxidation state of the Hf center is +2. In a square-pyramidal structure of idealized C_{4v} symmetry, the two lowest energy d orbitals will be a degenerate d_{xz} and d_{yz} pair, and a complex with a d^2 electronic configuration should be paramagnetic. The presence of the ethylene ligand in the axial site breaks the C_{4v} symmetry, and overlap with the π^* orbital of the ethylene ligand will split these two orbitals apart in energy and cause spin pairing of the two d electrons.

Anionic Ethylene Complex of Tantalum. Alkylation of $TaCl_2(OMe)_3$ with 8 equiv of LiEt in diethyl ether at −78 °C, followed by warming to room temperature and addition of tmed, affords small amounts of the tantalum(−I) hydrido/ethylene complex $[Li(tmed)]_3[TaHEt(C_2H_4)_3]\cdot{}^1/_2$tmed as red crystals.

$$TaCl_2(OMe)_3 + 8LiEt + 3.5tmed \rightarrow [Li(tmed)]_3[TaHEt(C_2H_4)_3]\cdot{}^1/_2tmed + 2LiCl + 3LiOMe + C_2H_4 + 3C_2H_6$$
2

The molecular structure of **2** is shown in Figure 3; crystal data and selected bond distances and angles are given in Tables 1 and 3. The tantalum center is coordinated to one hydride, one ethyl group,[55] and three ethylene ligands. If each ethylene ligand is considered to occupy one coordination site, the tantalum center adopts a distorted-square-pyramidal geometry

(41) Takashi, T.; Tamura, M.; Saburi, M.; Uchida, Y.; Negishi, E. *J. Chem. Soc., Chem. Commun.* **1989**, 852–853.
(42) Alt, H. G.; Denner, C. E.; Thewalt, T.; Rausch, M. D. *J. Organomet. Chem.* **1988**, *356*, C83–C85.
(43) Takashi, T.; Murakami, M.; Kunishige, M.; Saburi, M.; Uchida, Y.; Kozawa, K.; Uchida, T.; Swanson, D.; Negishi, E. *Chem. Lett.* **1989**, *761*, 764.
(44) Krüger, K.; Muller, G.; Erker, G.; Dorf, U.; Engel, K. *Organometallics* **1985**, *4*, 215–223.
(45) Cotton, F. A.; Kibala, P. A. *Inorg. Chem.* **1990**, *29*, 3192–3196.
(46) Mann, B. E.; Taylor, B. F. *^{13}C NMR Data for Inorganic Compounds*; Academic: New York, 1981; Table 2.10.
(47) Andersen, R. A. *Inorg. Chem.* **1979**, *18*, 2928–2932.
(48) Andersen, R. A. *J. Organomet. Chem.* **1980**, *192*, 189–193.
(49) Lancaster, S. J.; Robinson, O. B.; Bochmann, M.; Coles, S. J.; Hursthouse, M. B. *Organometallics* **1995**, *14*, 2456–2462.
(50) Schrock, R. R.; Baumann, R.; Reid, S. M.; Goodman, J. T.; Stumpf, R.; Davis, W. M. *Organometallics* **1999**, *18*, 3649–3670.
(51) Liang, L.-C.; Schrock, R. R.; Davis, W. M. *Organometallics* **2000**, *19*, 2526–2531.
(52) Mehrkhodavandi, P.; Schrock, R. R. *J. Am. Chem. Soc.* **2001**, *123*, 10746–10747.
(53) Alt, H. G.; Denner, C. E.; Milius, W. *Inorg. Chim. Acta* **2004**, *357*, 1682–1694.
(54) Spencer, L. P.; Fryzuk, M. D. *J. Organomet. Chem.* **2005**, *690*, 5788–5803.

(55) We considered whether the axial ethyl group is actually a methoxide ligand retained from the $TaCl_2(OMe)_3$ starting material. Attempts to refine these atoms as a methoxide group led to unreasonably large displacement parameters for the oxygen atom. Furthermore, we believe that this alternative can be ruled out on chemical grounds: if a methoxide group were actually present, the lithium cations would almost certainly interact with the partial negative charge on the oxygen atom. Instead, the preference of the lithium cations to form bonds exclusively to the ethylene and hydride ligands strongly suggests that the other axial ligand does not bear a significant negative charge.

with the hydride ligand in the axial site. The C−C vectors of all three C_2H_4 ligands are essentially parallel to the Ta−H vector. The Ta−C distances for the C_2H_4 groups are nearly identical and average at 2.267(16) Å. The two ethylene ligands that are cis to the Ta−Et group are each involved in interactions with the $[Li(tmed)]^+$ cations: one cation bridges between these two C_2H_4 ligands and the other two cations bridge between a C_2H_4 group and the hydride group. The Li···C distances involving these C_2H_4 groups lie in the narrow range 2.229(15)–2.316(15) Å. Taken together, these groups form a cyclic Li−C=C−Li−H−Li−C=C girdle about the tantalum center. The lithium cation that bridges between the two ethylene ligands also forms a weak interaction with the third ethylene, which is trans to the Ta−Et group; the Li···C distances for the axial C_2H_4 group of 2.502(15) Å is relatively long. The C−C distance of 1.484(8) Å for the third C_2H_4 group is slightly shorter than those of 1.515(8) and 1.502(8) Å for the two C_2H_4 groups that are involved in a strong interaction with the lithium centers.

A few other tantalum complexes containing C_2H_4 groups have been structurally characterized: among these are the metallocenes $Cp_2TaH(C_2H_4)\cdot AlEt_3$[56] and $[Me_2Si(C_5Me_4)_2]TaH(C_2H_4)$,[57] the half-sandwich complexes $CpTaCl_2(C_2H_4)(PMe_2Ph)_2$,[58] $Cp^*Ta(=NP(CMe_3)_3)Cl(C_2H_4)$,[59] $Cp^*Ta[=N(2,6\text{-}C_6H_3Me_2)](C_2H_4)(PMe_3)$,[60] and $Cp^*Ta(=CHCMe_3)(C_2H_4)(PMe_3)$,[61] and the non-cyclopentadienyl complexes $Ta(P_2N_2)Et(C_2H_4)$,[62] $Ta(CNN)(OCMe_3)(C_2H_4)$,[63] and $Ta(F_3N_2NMe)Et(C_2H_4)$,[64] where P_2N_2 = $PhP(CH_2SiMe_2NSiMe_2CH_2)_2PPh$, CNN = $C_6H_4(2\text{-}CH_2N(Me)CH_2CH_2NMe_2)$, and F_3N_2NMe = $(3,4,5\text{-}F_3C_6H_2\text{-}NCH_2CH_2)_2NMe$. The average Ta−C distance of 2.267(16) Å in **2** lies in the range seen in these tantalum ethylene complexes. In contrast, the C−C bond lengths in the ethylene groups in **2** are all significantly longer than those of 1.449(5)−1.502(9) Å in these other Ta−ethylene species, probably because the ethylene ligands in **2** are also involved in bonding interactions with the Li(tmed) units.

The Ta−H distance of 2.07(9) Å is significantly longer than analogous distances reported for other tantalum hydride complexes.[65–68] This longer Ta−H distance in **2** presumably reflects the presence of close Li···H contacts of 1.92(6) and 1.99(7) Å. The hydride ligand is displaced out of the equatorial plane toward the axial ethyl group: the angle between the Ta−H vector and the equatorial plane is 28.6°. This displacement minimizes the steric repulsion between the hydride and the axial ethylene ligand.

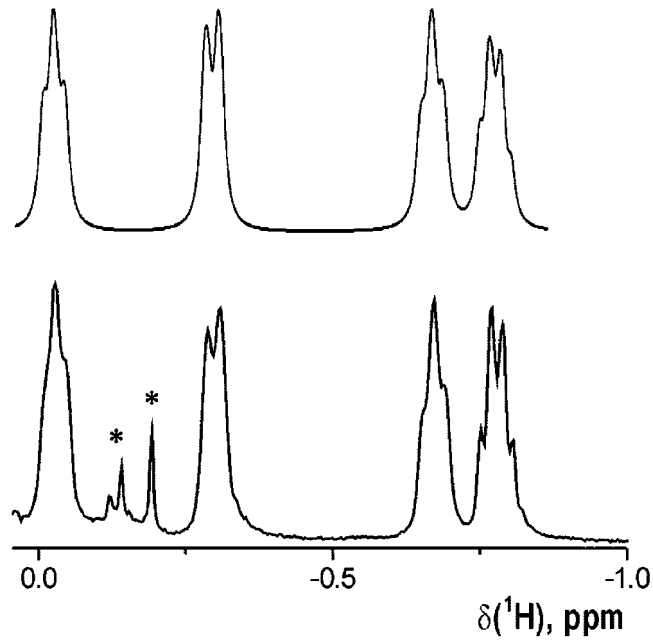

Figure 4. Experimental (lower) and simulated (upper) 500 MHz ^1H NMR spectra at −80 °C of the nonrotating ethylene ligands in $[Li(tmed)]_3[TaHEt(C_2H_4)_4]\cdot{}^1/_2tmed$ (**2**). Asterisks indicate peaks due to impurities. For chemical shifts and coupling constants, see the Experimental Section.

The ^1H NMR spectrum of **2** at −80 °C contains five resonances between δ 0.1 and −0.8 due to the ethylene ligands. A sharp singlet at δ 0.15 of intensity 4 is assigned to the axial ethylene group, which evidently is rotating rapidly on the NMR time scale about its Ta−C_2H_4 axis. A doublet, two triplets, and a quartet all of intensity 2 (all of which show deviations from binomial intensities due to second-order effects) correspond to an ABCD spin system (Figure 4). These four resonances are assigned to the two equatorial ethylene ligands, which are equivalent by symmetry and must be static (nonrotating) on the NMR time scale. No resonance was evident for the Ta−H group at negative chemical shifts, but there is a broad resonance at δ 1.23 of intensity 1; we tentatively assign this resonance to the Ta−H group. Warming the sample causes small shifts in peak locations, but no coalescence or broadening occurs that would indicate exchange between the inequivalent ethylene sites or between the ethylene and hydride environments.

The electronic structure of **2** will be discussed below in conjunction with that of the structurally similar tungsten complex.

Anionic Ethylene Complex of Tungsten. We have been unable to isolate products from the addition of ethyllithium to WCl_6, but alkylation of $WCl_3(OMe)_3$[69] with 9 equiv of LiEt in diethyl ether at −78 °C, followed by warming to room temperature and addition of tmed, gives yellow-orange crystals with the stoichiometry $[Li(tmed)]_3[WH(C_2H_4)_4]$ (**3**). This product is water-sensitive.

(56) McDade, C.; Gibson, V. C.; Santarsiero, B. D.; Bercaw, J. E. *Organometallics* **1988**, *7*, 1–7.
(57) Shin, J. H.; Parkin, G. *Chem. Commun.* **1999**, *887*, 888.
(58) Atwood, J. L.; Honan, M. B.; Rogers, R. D. *J. Crystallogr. Spectrosc. Res.* **1982**, *12*, 205–221.
(59) Courtenay, S.; Stephan, D. W. *Organometallics* **2001**, *20*, 1442–1450.
(60) Schultz, A. J.; Brown, R. K.; Williams, J. M.; Schrock, R. R. *J. Am. Chem. Soc.* **1981**, *103*, 169–176.
(61) Royo, P.; Sanchez-Nieves, J.; Pellinghelli, M. A.; Tiripicchio, A. *J. Organomet. Chem.* **1998**, *563*, 15–21.
(62) Fryzuk, M. D.; Johnson, S. A.; Rettig, S. J. *J. Am. Chem. Soc.* **2001**, *123*, 1602–1612.
(63) Rietveld, M. H. P.; Teunissen, W.; Hagen, H.; van de Water, L.; Grove, D. M.; van der Schaaf, P. A.; Muhlebach, A.; Kooijman, H.; Smeets, W. J. J.; Veldman, N.; Spek, A. L.; van Koten, G. *Organometallics* **1997**, *16*, 1674–1684.
(64) Lopez, L. P. H.; Schrock, R. R.; Bonitatebus, P. J., Jr *Inorg. Chim. Acta* **2006**, *359*, 4730–4740.
(65) Boni, G.; Blacque, O.; Sauvageot, P.; Poujaud, N.; Moise, C.; Kubicki, M. M. *Polyhedron* **2002**, *21*, 371–379.
(66) Nikonov, G. I.; Kuzmina, L. G.; Mountford, P.; Lemenovskii, D. A. *Organometallics* **1995**, *14*, 3588–3591.
(67) Arkhireeva, T. M.; Bulychev, B. M.; Protsky, A. N.; Soloveichik, G. L.; Bel'sky, V. K. *J. Organomet. Chem.* **1986**, *317*, 33–40.
(68) Wilson, R. D.; Koetzle, T. F.; Hart, D. W.; Kvick, A.; Tipton, D. L.; Bau, R. *J. Am. Chem. Soc.* **1977**, *99*, 1775–1781.
(69) Handy, L. B.; Sharp, K. G.; Brinckman, F. E. *Inorg. Chem.* **1972**, *11*, 523–531.

$$WCl_3(OMe)_3 + 9LiEt + 3tmed \rightarrow [Li(tmed)]_3[WH(C_2H_4)_4] + 3LiOMe + 3LiCl + C_2H_4 + 4C_2H_6$$

3

The synthesis of $[WH(C_2H_4)_4^{3-}]$ follows the analogous reaction of tungsten(VI) salts with methyllithium, which affords the octamethyltungstate ion $[WMe_8^{2-}]$.[70]

Single crystals of **3** were grown from Et_2O at −20 °C. Crystal data are given in Table 1, and selected bond distances and angles are given in Table 4. The overall structure of **3** closely resembles that of the tantalum ethylene complex **2**: the geometry about the tungsten center is a distorted square pyramid with the hydride ligand in the axial site (Figure 5). As for the tantalum complex **2**, two of the ethylene ligands, the hydride, and the three $[Li(tmed)]^+$ cations form a cyclic Li−C═C−Li−H−Li−C═C girdle about the metal center. One $[Li(tmed)]^+$ group bridges between the two ethylene ligands, and the other two $[Li(tmed)]^+$ ligands bridge between an ethylene group and the hydride ligand. The Li···C distances to these ethylene ligands range from ca. 2.16 to 2.20 Å. The two other C_2H_4 ligands are engaged in much weaker interactions with the Li centers: carbon atoms C(5), C(7), and C(8) exhibit longer-ranged Li···C contacts of 2.66 Å, and there are no significant Li···C contacts to carbon atom C(6). These two ethylene ligands are staggered with respect to one another when viewed down the ethylene−W−ethylene axis. Presumably, this conformation is adopted so as to minimize the competition for back-donation from the filled metal orbitals on tungsten (see below).

The W−C distances range from 2.182 to 2.244 Å and are within the range seen for other structurally characterized tungsten ethylene complexes. Only three other crystallographically characterized tungsten compounds are known that bear more than one ethylene ligand: $W(C_2H_4)_2(CO)_4$,[71] $W(C_2H_4)_2(PMe_3)_4$,[72] and $WClMe(C_2H_4)_2(PMe_3)_2 \cdot AlClMe_2$.[73] Tungsten ethylene complexes are thought to have significant metal−ethylene back-donation, because the W−C distances are comparable to those found in tungsten−ethyl complexes.[74–78] The C(5)−C(6) bond distance in **3**, 1.357(11) Å, is the shortest in the molecule and is only 0.020 Å longer than the C−C distance reported for free ethylene.[79,80] The C−C bond distances in the remaining three ethylene groups, 1.463(10), 1.466(10), and 1.447(11) Å, are significantly longer, probably because these ethylene groups are involved in Li···C contacts with the lithium cations.

Table 4. Selected Bond Distances and Angles for $[Li(tmed)]_3[WH(C_2H_4)_4]$ (3)

Bond Lengths (Å)			
W−H	2.04(5)	C(5)−C(6)	1.357(11)
W−C(1)	2.244(8)	C(7)−C(8)	1.447(11)
W−C(2)	2.208(7)	Li(1)−H	1.95
W−C(3)	2.229(7)	Li(2)−H	1.99
W−C(4)	2.233(7)	Li(1)−C(1)	2.18
W−C(5)	2.221(9)	Li(1)−C(7)	2.633(15)
W−C(6)	2.233(8)	Li(2)−C(3)	2.18
W−C(7)	2.197(8)	Li(2)−C(5)	2.72(2)
W−C(8)	2.182(8)	Li(3)−C(2)	2.20
C(1)−C(2)	1.463(10)	Li(3)−C(4)	2.16
C(3)−C(4)	1.466(10)	Li(3)−C(8)	2.619(14)
Bond Angles (deg)			
C(2)−W−C(1)	38.3(3)	C(7)−W−C(4)	105.1(3)
C(2)−W−C(3)	137.4(3)	C(7)−W−C(5)	146.5(4)
C(2)−W−C(4)	100.5(3)	C(7)−W-C(6)	151.9(4)
C(2)−W−C(5)	109.1(4)	C(8)−W-C(1)	85.1(3)
C(2)−W−C(6)	78.5(3)	C(8)−W-C(2)	80.2(3)
C(3)−W−C(1)	165.6(3)	C(8)−W−C(3)	80.5(3)
C(3)−W−C(4)	38.4(3)	C(8)−W−C(4)	79.0(3)
C(3)−W−C(6)	113.9(3)	C(8)−W−C(5)	157.6(4)
C(4)−W−C(1)	138.2(3)	C(8)−W−C(6)	158.6(3)
C(4)−W−C(6)	102.2(4)	C(8)−W−C(7)	38.6(3)
C(5)−W−C(1)	115.1(3)	C(1)−W−H	90.8(15)
C(5)−W−C(3)	79.1(3)	C(2)−W−H	125.3(15)
C(5)−W−C(4)	79.3(3)	C(3)−W−H	97.0(15)
C(5)−W−C(6)	35.5(3)	C(4)−W−H	130.2(15)
C(6)−W−C(1)	80.0(3)	C(5)−W−H	68.6(15)
C(7)−W−C(1)	84.1(3)	C(6)−W−H	72.4(15)
C(7)−W−C(2)	102.8(4)	C(7)−W−H	84.8(15)
C(7)−W−C(3)	84.5(3)	C(8)−W−H	123.4(15)

The W−H distance of 2.04(5) Å is one of the longest W−H distances reported.[81–83] The long distance is probably a consequence of the low formal oxidation state of the tungsten atom and the presence of two close contacts of 1.97 Å between the hydride ligand and the lithium cations. The Li···H contact distances in compound **3** are within the 1.73(6)–2.02(5) range seen for $\{Li[WH_5(PMe_3)_3]\}_4$.[82] Interestingly, the hydride ligand is displaced by 0.24 Å out of the mean plane of the cyclic Li−C═C−Li−H−Li−C═C girdle: it is tilted toward the C(5)−C(6) ethylene group by 20.5°. The displacement of the hydride ligand out of the girdle plane minimizes the steric repulsion with atom C(7).

The ^{1}H NMR spectrum of **3** in tetrahydrofuran-d_8 at –80 °C contains three broad ethylene resonances at δ –0.38, –0.79, and –1.27 with intensities 8:4:4, respectively, and a high-field resonance at δ –8.21 due to the hydride ligand (Figure 6). The presence of three resonances due to the ethylene ligands suggests that the two ethylene ligands not involved in strong interactions with the lithium centers are rotating rapidly about the W−C_2H_4 bonds even at low temperatures, but the other two ethylene ligands are static. The low rotation barriers for the latter C_2H_4 groups reflect the presence of a pair of filled π-bonding orbitals on the tungsten center (see below). At –30 °C, the hydride resonance sharpens slightly and the observed tungsten-to-hydride coupling constant, $J_{WH} = 69.1$ Hz, is within the 28–80 Hz range seen for other tungsten hydride complexes.[84]

As the sample is warmed, the three signals due to the ethylene ligands broaden and coalesce. At room temperature, the

(70) Galyer, A. L.; Wilkinson, G. *J. Chem. Soc., Dalton Trans.* **1976**, 2235–2238.
(71) Szymanska-Buzar, T.; Kern, K.; Downs, A. J.; Greene, T. M.; Morris, L. J.; Parsons, S. *New J. Chem.* **1999**, *23*, 407–416.
(72) Carmona, E.; Galindo, A.; Poveda, M. L.; Rogers, R. D. *Inorg. Chem.* **1985**, *24*, 4033–4039.
(73) Sharp, P. R. *Organometallics* **1984**, *3*, 1217–1223.
(74) Barry, J. T.; Chacon, S. T.; Chisholm, M. H.; Huffman, J. C.; Streib, W. E. *J. Am. Chem. Soc.* **1995**, *117*, 1974–1990.
(75) Carmichael, A. J.; McCamley, A. *J. Chem. Soc., Dalton Trans.* **1995**, 3125–3129.
(76) Chisholm, M. H.; Putilina, E. F.; Folting, K.; Streib, W. E. *J. Cluster Sci.* **1994**, *5*, 67–82.
(77) Eagle, A. A.; Young, C. G.; Tiekink, E. R. T. *Organometallics* **1992**, *11*, 2934–2938.
(78) Chisholm, M. H.; Chiu, H. T.; Huffman, J. C.; Wang, R. J. *Inorg. Chem.* **1986**, *25*, 1092–1096.
(79) Bartell, L. S.; Roth, E. A.; Hollowell, C. D.; Kuchitsu, K.; Young, J. E. Jr. *J. Chem. Phys.* **1965**, *42*, 2683–2686.
(80) It is possible that librational motion of this ethylene ligand affects the measured C−C distance and that the true C−C distance for this ligand is somewhat longer.
(81) Piana, H.; Schubert, U. *J. Organomet. Chem.* **1991**, *411*, 303–323.
(82) Barron, A. R.; Wilkinson, G.; Motevalli, M.; Hursthouse, M. B. *J. Chem. Soc., Dalton Trans.* **1987**, 837–846.
(83) Park, J. T.; Shapley, J. R.; Chuchill, M. R.; Bueno, C. *Inorg. Chem.* **1984**, *23*, 4476–4486.
(84) Jesson, J. P. In *Transition Metal Hydrides*; Muetterties, E. L., Ed.; Dekker: New York, 1971; Chapter 4.

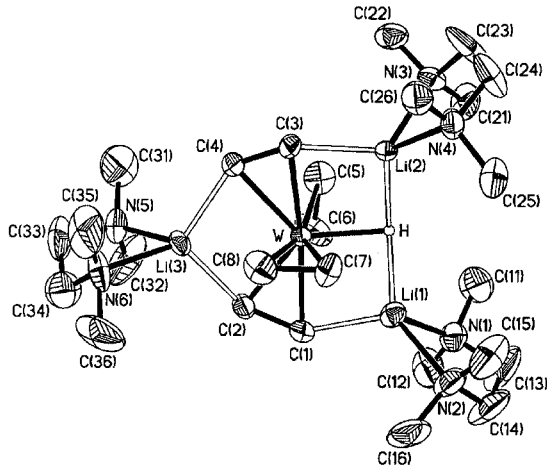

Figure 5. Molecular structure of $[Li(tmed)]_3[WH(C_2H_4)_4]$ (**3**). The ellipsoids represent the 30% probability density surfaces, except for hydrogen atoms, which are represented by arbitrarily sized spheres.

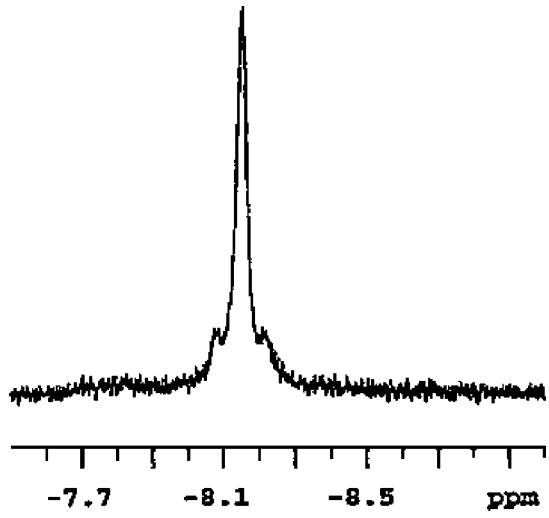

Figure 6. 500 MHz ^{1}H NMR spectrum of the W−H resonance of $[Li(tmed)]_3[WH(C_2H_4)_4]$ (**3**) in thf-d_8 at –30 °C showing the $^1J_{WH}$ coupling.

spectrum consists of one sharp singlet at δ –0.66 for the protons of the four ethylene groups and one signal for the hydride ligand at δ −8.14. Correspondingly, the $^{13}C\{^1H\}$ NMR spectrum of **3** at low temperature (Figure 7) contains three resonances at δ 35.1, 19.7, and 18.3 for the ethylene ligands, whereas the room-temperature spectrum shows one singlet at δ 26.9 for all four ethylene groups. We attribute the changes in the NMR spectra to an exchange process involving only the ethylene ligands.

The line shapes of the ethylene proton resonances were compared with computer-generated spectra to determine the exchange rate (Figure 8). The activation parameters[85] $\Delta H^{\ddagger} =$ 9.5(10) kcal mol^{-1} and $\Delta S^{\ddagger} = -5(4)$ cal mol^{-1} K^{-1} for this exchange process were calculated from an Eyring plot (Figure 9). Presumably, the interconversion of the ethylene ligands involves movement of the lithium interactions from one pair of ethylene ligands to the other, along with a rearrangement of the interligand angles that is analogous to a Berry pseudorotation mechanism[86] in which the hydride ligand is the pivot atom. The tantalum compound **2** does not show this type of fluxional behavior, because the presence of the ethyl group breaks the symmetry (two ethylene ligands are cis to the ethyl group and one is trans), and a different (and higher energy) transition state is necessary to effect exchange.

Interestingly, variable-temperature NMR spectroscopy shows that the hydride resonance in **3** is broad at −90 °C (59 Hz), is narrowest near –10 °C (15 Hz), and is broad again at room temperature (53 Hz). A spin saturation transfer experiment was conducted, which showed that chemical exchange between the W−H and W−C_2H_4 environments is not occurring on the NMR time scale, even at temperatures as high as 40 °C. The changes in the line width of the W−H resonances as a function of temperature probably reflect temperature-dependent ion-pairing equilibria between the $[Li(tmed)^+]$ cations and the $[WH(C_2H_4)_4{}^{3-}]$ anions.

Electronic Structures of 2 and 3. The diamagnetism of the tungsten compound **3** can be rationalized on several grounds. First, the complex has an electron count of 18 and the metal is surrounded by strong-field ligands; in such cases, diamagnetism is almost invariably the result. A more precise picture of the electronic structure and details of the structure of **3** can be obtained either in terms of a trigonal-bipyramidal or square-pyramidal arrangement of ligands. Although both views lead to similar results, it is slightly more useful to interpret the electronic structure in terms of a square-pyramidal coordination geometry, with the hydride ligand in the axial site (i.e., with the Ta−H vector pointing along the z axis). From this perspective, the idealized d-orbital splitting pattern would be $(d_{xz}, d_{yz}) < d_{xy} < d_{z^2} < d_{x^2-y^2}$ (Figure 10). For tungsten(−II), a d^8 complex, all the orbitals except the highest energy $d_{x^2-y^2}$ will be filled. Further stabilization of the filled orbitals on tungsten will result from π-back-bonding with the empty π^* orbitals on the ethylene ligands. If the plane of the cyclic Li−C═C−Li−H−Li−C═C girdle is defined as the xz plane, then the two ethylene ligands in this plane both interact with the d_{xz} orbital. The C−C vectors of the two ethylene ligands that lie along the y axis are staggered with respect to each other, and this structural feature reflects the fact that one of these ligands engages in π-back-bonding with the d_{yz} orbital and the other with the d_{xy} orbital. This idealized view of the bonding will change slightly upon increasing the angle between the axial hydride ligand and the four equatorial ethylene ligands from 90° as seen experimentally, but the basic features will be unchanged.

The tantalum complex **2** has a formal oxidation state of −1 and thus has a d^6 electronic configuration. In terms of the same square-pyramidal geometry, the diamagnetism is accounted for by filling the $(d_{xz}, d_{yz}) < d_{xy} < d_{z^2} < d_{x^2-y^2}$ splitting diagram only to the d_{xy} level. The bonding between the tantalum center and the ethylene ligands, however, can be described in a way very similar to that in the tungsten complex.

Experimental Section

All operations were performed under vacuum or under argon by using Schlenk and cannula methods. Diethyl ether and methanol were distilled immediately before use from sodium benzophenone and magnesium, respectively. $HfCl_4$, $TaCl_5$, and WCl_6 were obtained from Cerac and were sublimed under vacuum. Ethyllithium was prepared according to literature methods.[87] *N*,*N*,*N*′,*N*′-Tetramethylethylenediamine (Aldrich) was distilled from sodium. Tetrahydrofuran-d_8 (Cambridge Isotope Laboratories) was dried over

(85) NMR studies show that the ethylene exchange barrier decreases with decreasing tmed concentration. We conclude that the Li···C contacts present in the solid-state structure of **1** promote the ethylene fluxional behavior.

(86) Alvarez, S.; Llunell, M. *Dalton Trans.* **2000**, 3288–3303.

(87) Bryce-Smith, D.; Turner, E. E. *J. Chem. Soc.* **1953**, 861–867.

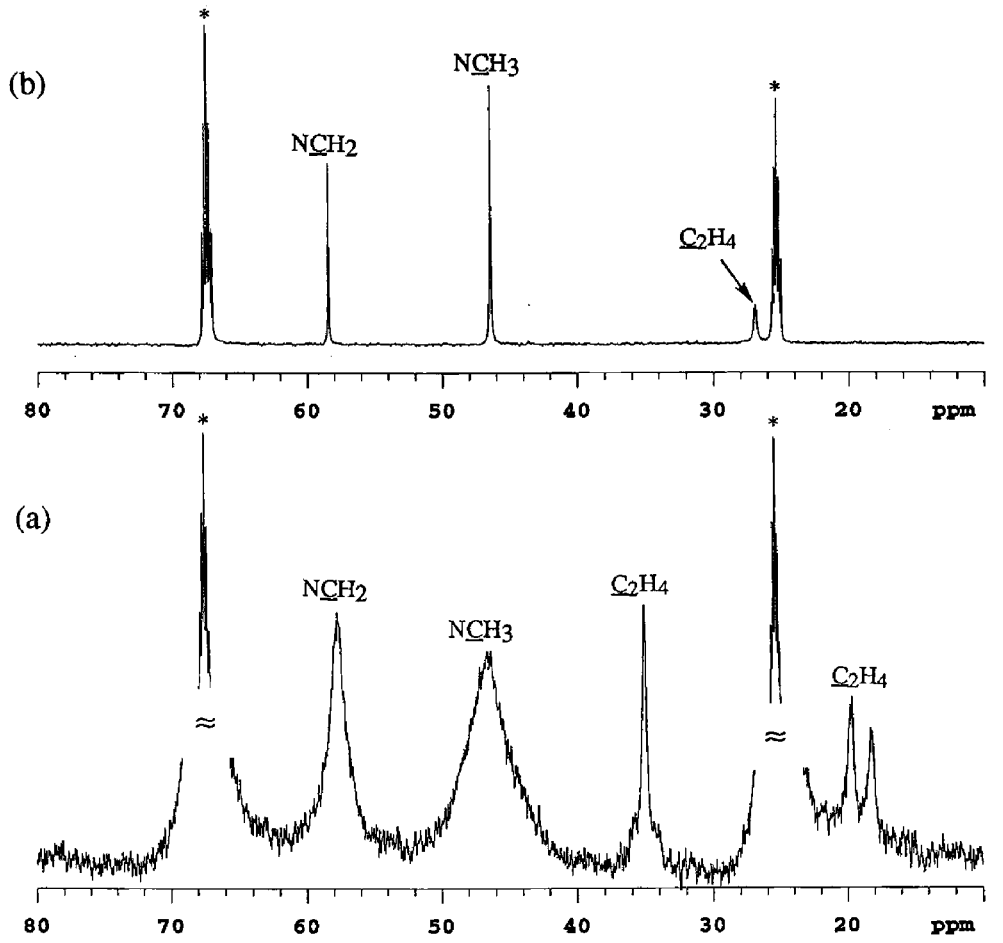

Figure 7. 125 MHz $^{13}C\{^1H\}$ NMR spectrum of $[Li(tmed)]_3[WH(C_2H_4)_4]$ (**3**) in thf-d_8 at (a) –90 °C and (b) 20 °C. Asterisks indicate peaks due to solvent.

alumina before use. IR spectra were recorded on a Perkin-Elmer 599B grating instrument or a Nicolet Impact 410 Fourier transform spectrometer as Nujol mulls between KBr salt plates. The solution NMR data were recorded on a General Electric QE-300 instrument or on a General Electric GN-300 NB instrument at 300 MHz (^1H) or 75.44 MHz (^{13}C); some spectra were acquired on a Varian U500 spectrometer at 500 MHz (^1H) or 125 MHz (^{13}C). The temperature of the NMR probe was calibrated with methanol (for low temperatures) or ethylene glycol (for high temperatures),[88,89] and the estimated relative error in the temperature measurements was 0.3 K. Solid-state CPMAS ^{13}C NMR data were collected on a General Electric GN-300 instrument with a 2 ms pulse width, a 10 s interpulse delay, a 20 000 Hz window, a 2500−3000 Hz spinning rate, and a 2K data storage size. Samples were packed under an inert atmosphere into Kel-F rotors that were modified for air-sensitive samples.[90] Chemical shifts are reported in δ units (positive shifts to high frequency) relative to tetramethylsilane. Simulations of NMR line shapes were carried out with the program NUTS (Acorn NMR), DNMR (Quantum Chemistry Program Exchange), DNMR3H (Quantum Chemistry Program Exchange), or WINDNMR (Journal of Chemical Education Software). Microanalyses were performed by the Microanalytical Laboratory in the School of Chemical Sciences at the University of Illinois.

Bis[(*N*,*N*,*N*′,*N*′-tetramethylethylenediamine)lithium] Tetraethyl(ethylene)hafnate(II), $[Li(tmed)]_2[HfEt_4(C_2H_4)]$ (1). To a suspension of $HfCl_4$ (0.88 g, 2.7 mmol) in diethyl ether (70 mL) at −78 °C was added a solution of ethyllithium (0.60 g, 16 mmol) in diethyl ether (20 mL). The solution was warmed to 0 °C and was stirred for 2 h. The solution was filtered at 0 °C, and *N*,*N*,*N*′,*N*′-tetramethylethylenediamine (0.8 mL, 5.4 mmol) was added to the filtrate. The solution was concentrated to ca. 50 mL and cooled to −20 °C to yield colorless crystals. Yield: 0.9 g (60%). Mp: 105 °C dec. Anal. Calcd for $C_{22}H_{56}N_4Li_2Hf$: C, 46.4; H, 9.9; N, 9.8; Li, 2.4. Found: C, 46.3; H, 9.8; N, 9.8; Li, 2.8. ^1H NMR (C_7D_8, 20 °C): δ 0.05 (q, J_{HH} = 7.5 Hz, 8 H, Hf−CH_2Me), 0.31 (s, 4H, Hf−C_2H_4), 1.70 (s, 8H, NCH_2), 2.00 (s, 24H, NMe_2), 2.06 (t, J_{HH} = 7.5 Hz, 12H, Hf−CH_2Me). ^{13}C NMR (C_7D_8, 20 °C): δ 13.8 (q, J_{CH} = 121 Hz, 4C, Hf−CH_2Me), 31.0 (t, J_{CH} = 120 Hz, 2C, Hf−C_2H_4), 41.9 (t, J_{CH} = 106 Hz, 4C, Hf−CH_2Me), 45.9 (q, J_{CH} = 132 Hz, 8C, NMe_2), 56.5 (t, J_{CH} = 136 Hz, 4C, NCH_2). $^{13}C\{^1H\}$ NMR (CPMAS, −50 °C): δ 13.8 (s, 1C, CH_2Me), 14.8 (s, 2C, CH_2Me), 16.8 (s, 1C, CH_2Me), 32.0 (s, 2C, Hf−C_2H_4), 34.0 (s, 1C, CH_2Me), 46.7 (s, 4C, NMe_2), 48.1 (s, 4C, NMe_2), 52.1 (s, 1C, CH_2Me), 57.7 (s, 4C, NCH_2). IR (cm^{-1}): 1410 w, 1357 m, 1291 s, 1252 w, 1181 w, 1158 m, 1130 m, 1099 m, 1068 m, 1036 s, 1020 s, 1002 m, 950 s, 902 m, 792 s, 773 w, 723 w, 586 w, 535 m, 461 m, 439 m, 417 m, 402 m.

Dichlorotri(methoxy)tantalum(V), $TaCl_2(OMe)_3$.[91] To $TaCl_5$ (2.10 g, 5.9 mmol) was added degassed methanol (45 mL). The reaction mixture, which became warm, was stirred at room temperature for 4 h. The clear solution was filtered, and the solvent was removed under vacuum to give a white solid. Yield: 1.81 g (89%). Anal. Calcd for $C_3H_9O_3Cl_2Ta$: C, 10.4; H, 2.61; Cl, 20.6, Ta, 52.5. Found: C, 9.50; H, 2.65; Cl, 21.0; Ta, 50.0.

(88) Friebolin, H.; Schilling, G.; Pohl, L. *Org. Magn. Reson.* **1979**, *12*, 569–573.
(89) Van Geet, A. L. *Anal. Chem.* **1970**, *42*, 679–680.
(90) Haw, J. F.; Speed, J. A. *J. Magn. Reson.* **1988**, *78*, 344–347.
(91) Funk, H.; Niederlander, K. *Ber. Dtsch. Chem. Ges. B* **1929**, *62*, 1688–1691.

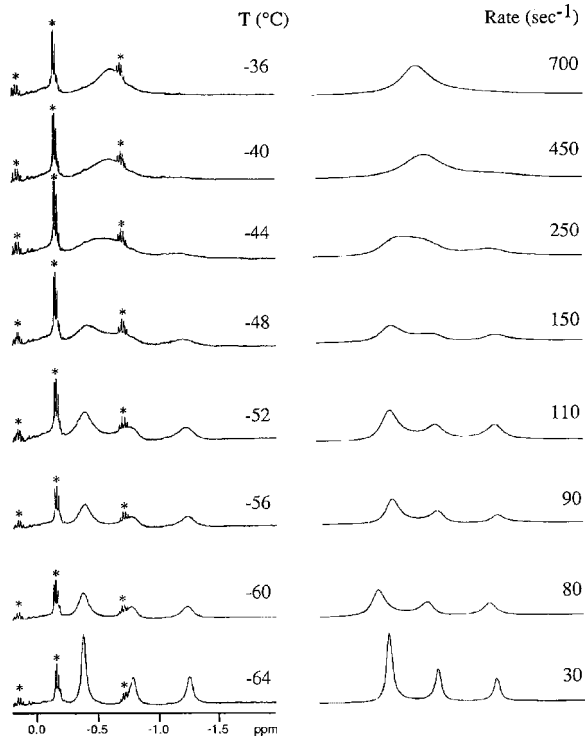

Figure 8. Variable-temperature 500 MHz ^{1}H NMR spectrum (left) and simulated spectrum (right) of $[Li(tmed)]_3[WH(C_2H_4)_4]$ (**3**) in the coordinated ethylene region. Asterisks indicate peaks due to impurities.

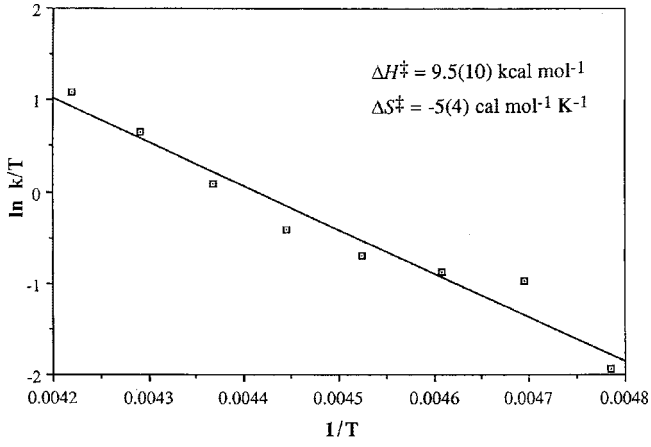

Figure 9. Eyring plot of the ethylene exchange process in $[Li(tmed)]_3[WH(C_2H_4)_4]$ (**3**).

Tris[(*N*,*N*,*N*′,*N*′-tetramethylethylenediamine)lithium] Hydrido(ethyl)tetrakis(ethylene)tantalum(−I), $[Li(tmed)]_3[TaHEt(C_2H_4)_4]\cdot {}^1/_2$tmed (2). To a suspension of $TaCl_2(OMe)_3$ (0.5 g, 1.4 mmol) in Et_2O (30 mL) at −78 °C was added a solution of LiEt (0.42 g, 11.7 mmol) in Et_2O (30 mL). The reaction mixture was stirred at −78 °C for 30 min and warmed to room temperature. The red solution was filtered from a white precipitate, and the filtrate was treated with *N*,*N*,*N*′,*N*′-tetramethylethylenediamine (1.3 mL). The red solution was concentrated to 25 mL, filtered, and kept at −20 °C for 10 days. The red solution was refiltered from additional white precipitate, concentrated to 5 mL, and cooled to −20 °C to afford a small number of red prisms. ^{1}H NMR (thf-d_8, −60 °C): δ −0.78 ("q", J_{HH} = 10.0, 9.0, 7.5 Hz, C_2H_4), −0.71 ("t", J_{HH} = 9.0, 8.0, 3.0 Hz, C_2H_4), −0.27 ("d", J_{HH} = 10.0, 3.0, 3.0 Hz, C_2H_4), 0.06 ("t", J_{HH} = 8.0, 7.5, 3.0 Hz, C_2H_4), 0.15 (s, C_2H_4), 1.23 (br, Ta−H?), 2.14 (s, NMe_2), 2.28 (s, NCH_2).

Trichlorotrimethoxytungsten(VI), $W(OMe)_3Cl_3$.[69] To a slurry of WCl_6 (4.0 g, 10 mmol) in pentane (50 mL) was added $MeOSiMe_3$ (8.3 mL, 60 mmol). The solution color changed from red to pale yellow over 45 min. The solution was filtered and cooled to −20 °C for 4 h to afford pale yellow crystals of $W(OMe)_3Cl_3$. Yield: 2.22 g (58%). Anal. Calcd for $C_3H_9O_3Cl_3W$: C, 9.40; H, 2.37; Cl, 27.7. Found: C, 9.52; H, 2.35; Cl, 25.6.

Tris[(*N*,*N*,*N*′,*N*′-tetramethylethylenediamine)lithium] Hydridotetrakis(ethylene)tungsten(−II), $[Li(tmed)]_3[WH(C_2H_4)_4]$ (3). To a solution of $W(OMe)_3Cl_3$ (0.25 g, 0.65 mmol) in Et_2O (10 mL) at −78 °C was added a solution of LiEt (0.235 g, 6.50 mmol) in Et_2O (20 mL) at −78 °C. The solution color changed from pale yellow to pale blue to pale green to brown-yellow within 1 min. The solution was stirred for 1 h at −78 °C and then was warmed to room temperature and stirred for another 2 h. The solution was filtered, concentrated to 20 mL, and then treated with freshly distilled *N*,*N*,*N*′,*N*′-tetramethylethylenediamine (1.00 mL). The solution was recooled to –78 °C, filtered, and kept at −20 °C for 6 h to afford yellow-orange crystals of **3**. Yield: 0.0215 g (5%). Anal. Calcd for $C_{26}H_{65}N_6WLi_3$: C, 46.8; H, 9.83; N, 12.6; W, 27.6; Li, 3.1. Found: C, 44.0; H, 9.11; N, 11.1; W, 26.7; Li, 3.1. ^{1}H NMR (thf-d_8, 17 °C): −8.14 (s, 1H, W−H), −0.66 (s, 16H, C_2H_4), 2.14 (s, 36H, NMe_2), 2.28 (s, 12H, NCH_2). ^{1}H NMR (thf-d_8, −80 °C): −8.21 (s, 1H, W−H), −1.27 (s, 4H, C_2H_4), −0.79 (s, 4H, C_2H_4), −0.38 (s, 8H, C_2H_4), 2.19 (s, 36H, NMe_2), 2.33 (s, 12H, NCH_2). ^{13}C NMR (thf-d_8, 17 °C): 26.9 (t, $^1J_{CH}$ = 137 Hz, C_2H_4), 46.4 (q, $^1J_{CH}$ = 137 Hz, NMe_2), 58.4 (t, $^1J_{CH}$ = 132 Hz, NCH_2). ^{13}C{^{1}H} NMR (thf-d_8, −80 °C): 18.3 (t, $^1J_{CH}$ = 131 Hz, 2C, C_2H_4), 19.7 (t, $^1J_{CH}$ = 136 Hz, 2C, C_2H_4), 35.1 (t, $^1J_{CH}$ = 140 Hz, 4C, C_2H_4), 46.3 (br s, NMe_2), 57.7 (br s, NCH_2). IR (cm^{-1}): 2791 (m), 2776 (m), 1537 (vw), 1531 (vw), 1519 (vw), 1514 (vw), 1504 (vw), 1494 (vw), 1456 (m), 1417 (w), 1403 (w), 1357 (w), 1291 (m), 1253 (vw), 1181 (vw), 1157 (w), 1129 (m), 1098 (w), 1069 (w), 1036 (m), 1022 (w), 947 (w), 791 (w), 773 (vw), 581 (vw), 535 (vw), 525 (vw), 516 (vw), 489 (vw), 470 (w), 454 (w), 446 (w), 438 (w).

Crystallographic Studies.[92] Single crystals of all three compounds, grown from diethyl ether, were mounted on glass fibers with Paratone-N oil (Exxon) and immediately cooled to –80 °C in a cold nitrogen gas stream on the diffractometer. Data were collected with an area detector by using the measurement parameters listed in Table 1. The measured intensities were reduced to structure factor amplitudes and their esd's by correction for background and Lorentz and polarization effects. Systematically absent reflections were deleted, and symmetry-equivalent reflections were averaged to yield the sets of unique data. The analytical approximations to the scattering factors were used, and all structure factors were corrected for both real and imaginary components of anomalous dispersion. All structures were solved using direct methods (SHELXTL) and subsequent Fourier difference calculations. Final refinement parameters are given in Table 1. Subsequent discussions for **1**−**3** will be divided into individual paragraphs.

$[Li(tmed)]_2[Hf(C_2H_4)Et_4]$ (1). Although we reported the crystal structure of this compound in our preliminary communication,[28] the data set was poor, and so we have recollected a much better data set on a new crystal. Systematic absences for 0*kl* ($k \neq 2n$), and *hk*0 ($h \neq 2n$) were consistent only with space group *Pbca*. The (1 0 2) reflection was obscured by beamstop and was deleted; the remaining 14 669 unique reflections were used in the least-squares refinement. The quantity minimized by the least-squares program was $\sum w(F_o^2 - F_c^2)^2$, where $w = \{[\sum(F_o^2)]^2 + (0.010P)^2\}^{-1}$ and $P = (F_o^2 + 2F_c^2)/3$. Methylene hydrogen atoms on the organic groups bound to hafnium were located in the difference maps, and their positions were refined with independent isotropic displacement parameters; the C−H distances to all these

(92) For details of the crystallographic methods used, see: Brumaghim, J. L.; Priepot, J. G.; Girolami, G. S. *Organometallics* **1999**, *18*, 2139–2144.

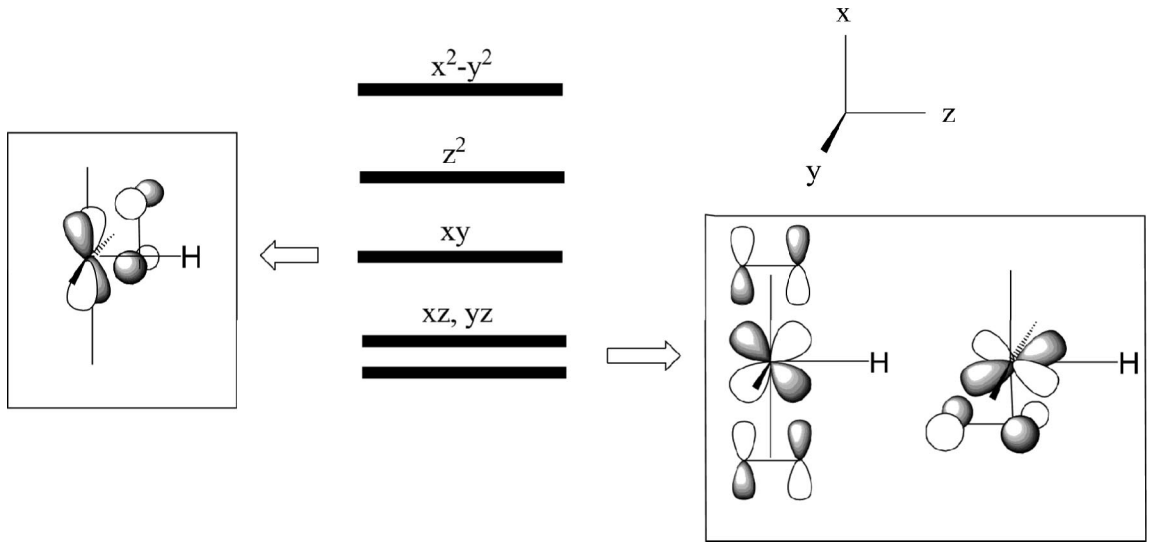

Figure 10. Orbital splitting diagram and π-back-bonding interactions to the ethylene ligands for $[Li(tmed)]_3[WH(C_2H_4)_4]$ (**3**).

hydrogens were constrained to be equal within 0.01 Å. Methyl hydrogens in the ethyl groups and all the hydrogen atoms in tmed groups were placed in idealized positions; the methyl groups were allowed to rotate about the C−C axis to find the best least-squares positions. The displacement parameters for idealized methylene hydrogens were set equal to 1.2 times U_{eq} for the attached carbon; those for methyl hydrogens were set to 1.5 times U_{eq}. Successful convergence was indicated by the maximum shift/error of 0.005 for the last cycle. Final refinement parameters are given in Table 1. The largest peak in the final Fourier difference map (1.21 e Å^{-3}) was located 1.35 Å from C16 and appears to be a "ghost" of the Hf atom; its location is related to that of Hf by the transformation $1 - x$, y, $0.5 - z$. A final analysis of variance between observed and calculated structure factors showed no apparent errors.

$[Li(tmed)]_3[TaHEt(C_2H_4)_4]\cdot{}^1/_2$tmed (2). Although highly suggestive of a *C*-centered monoclinic cell, the systematic absences actually were those of the primitive monoclinic space group $P2_1/c$, and this choice was confirmed by successful refinement of the proposed model. A total of 7272 unique data were used in the least-squares refinement. The quantity minimized by the least-squares program was $\sum w(F_o^2 - F_c^2)^2$, where $w = \{[\sigma(F_o^2)]^2 + (0.0352P)^2 + 0.06P\}^{-1}$ and $P = (F_o^2 + 2F_c^2)/3$. In the final cycle of least squares, anisotropic displacement factors were refined for the non-hydrogen atoms. The ethyl ligand was disordered over two sites and was refined as two ethyl groups (C(1A)−C(2A) and C(1B)−C(2B)), the major site having the site occupancy factor refined to 0.64(3). The C(1A)−C(2) and C(1B)−C(2B) distances in the disordered ethyl groups were constrained to be equal within 0.005 Å. The hydrogen atom attached to Ta was located in the difference maps, and its position was independently refined an isotropic displacement parameter. The other hydrogen atoms were fixed in "idealized" positions with C−H = 0.98 Å (methylene hydrogens) or 0.99 Å (methyl hydrogens), and their displacement parameters were set equal to 1.2 and 1.5 times U_{eq} for the attached carbon, respectively. No correction for isotropic extinction was necessary. Successful convergence was indicated by the maximum shift/error of 0.001 for the last cycle. The two largest peaks in the final Fourier difference map (both ~1.7 e Å^{-3}) were located 1.10 Å on opposite sides of the Ta atom and are clearly the result of errors in the absorption correction. A final analysis of variance between observed and calculated structure factors showed no apparent errors. The *C*-centered pseudosymmetry is the result of the location of the heavy Ta atom very near (¼, 0, ¼) such that the 2-fold screw corresponds very closely to a translation by ½, ½, 0.

$[Li(tmed)]_3[WH(C_2H_4)_4]$ (3). Systematic absences for $0kl$ ($k \neq 2n$), $h0l$ ($h \neq 2n$), and $hk0$ ($h \neq 2n$) were consistent only with space group *Pbca*. One reflection (0 0 2) was obscured by the beam stop and was deleted, and one reflection (4 16 6) had $I < -3\sigma(I)$ and was suppressed; the remaining 8691 unique data were used in the least-squares refinement. The quantity minimized by the least-squares program was $\sum w(F_o^2 - F_c^2)^2$, where $w = \{[\sigma(F_o^2)]^2 + (0.049P)^2\}^{-1}$ and $P = (F_o^2 + 2F_c^2)/3$. One carbon atom of a tmed ligand was clearly disordered over two sites and was refined as two isotropic partial atoms (C(34) and C(34A)); a site occupancy factor refined to 0.58(2) for the major site. The displacement parameters for some of the other tmed carbon atoms were somewhat large, but the electron density could be modeled satisfactorily without splitting these atoms over two sites. Some of the final distances within the tmed ligands, however (especially those involving the ethylene backbones), are affected by the unresolved disorder. Except for the W-bound hydride atoms, hydrogen atoms were placed in fixed positions with C−H = 0.99, 0.98 Å for CH_2 and CH_3 groups, respectively. Locations for the methyl hydrogen atoms were optimized by rotation about the C−X bond. Independent anisotropic displacement factors were refined for the non-hydrogen atoms. The W-bound hydrogen atom was assigned an individual isotropic displacement parameter, whereas the isotropic displacement parameters for the CH_2 and CH_3 hydrogen atoms were set equal to 1.2 times U_{eq} and 1.5 times U_{eq} for the attached carbon atoms, respectively. Corrections for crystal decay were unnecessary, but an empirical absorption correction was applied (SADABS), the maximum and minimum transmission factors being 0.801 and 0.510. Successful convergence was indicated by the maximum shift/error of 0.07 for the last cycle. The largest peak in the final Fourier difference map (0.99 e Å^{-3}) was located 0.94 Å from the tungsten atom. A final analysis of variance between observed and calculated structure factors showed no apparent errors.

Acknowledgment. We thank the National Science Foundation (Grants CHE 00-76061 and CHE 04-20768) for support of this work and Dr. Scott Wilson and Ms. Teresa Prussak-Wieckowska of the University of Illinois Materials Chemistry Laboratory for collecting the crystallographic data.

Supporting Information Available: X-ray crystallographic files in CIF format for $[Li(tmed)]_2[HfEt_4(C_2H_4)]$ (**1**), $[Li(tmed)]_3[TaHEt(C_2H_4)_4]\cdot$½tmed (**2**), and $[Li(tmed)]_3[WH(C_2H_4)_4]$ (**3**). This material is available free of charge via the Internet at http://pubs.acs.org.

OM701189E